# Supporting Information

## Achieving high-sensitive dual-mode optical thermometry via phonon-assisted cross-relaxation in double-perovskite structured up-conversion phosphor

Houhe Dong[a,1], Zonghao Lei[a,1], Shikun Su[a], Wenhua Yang [a*], Xuyang Zhang[a], Wenying Teng[a], Guangyue Zu[a], Bing Teng [a, b*], Degao Zhong[a, b, c*]

[a]College of Physics, University-Industry Joint Center for Ocean Observation and Broadband Communication, Qingdao University, Qingdao 266071, China,

[b]Qingdao Broadband Terahertz Spectroscopy Technology Engineering Research Center (Qingdao University), Qingdao 266071, China

[c]Weihai Innovation Research Institute of Qingdao University, Weihai 264200, China

[1] These authors contributed equally to this work

[*] Corresponding author.

Email: yangwh@qdu.edu.cn (Wenhua Yang), 5108tb@163.com (Bing Teng), zhdg2008@126.com (Degao Zhong)

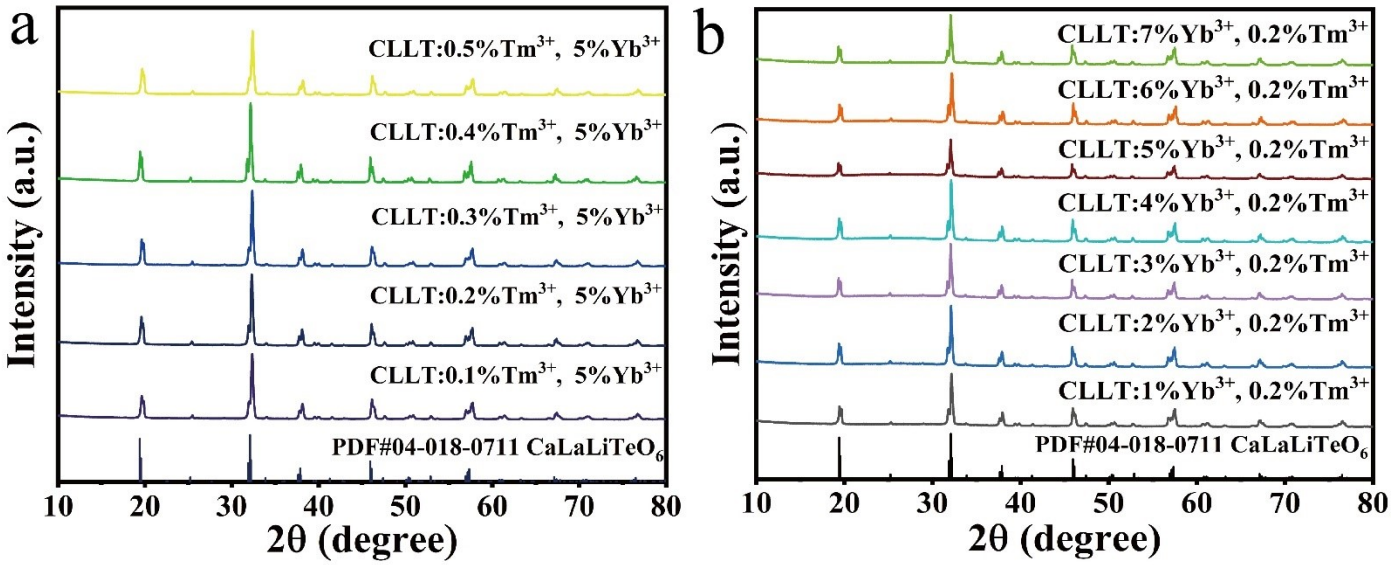


**Fig. S1.** (a and b) XRD profiles of $CaLaLiTeO_6$: $xTm^{3+}$, $5\%Yb^{3+}$ and $CaLaLiTeO_6$: 0.2% $Tm^{3+}$, $xYb^{3+}$ phosphors with diverse doping contents.

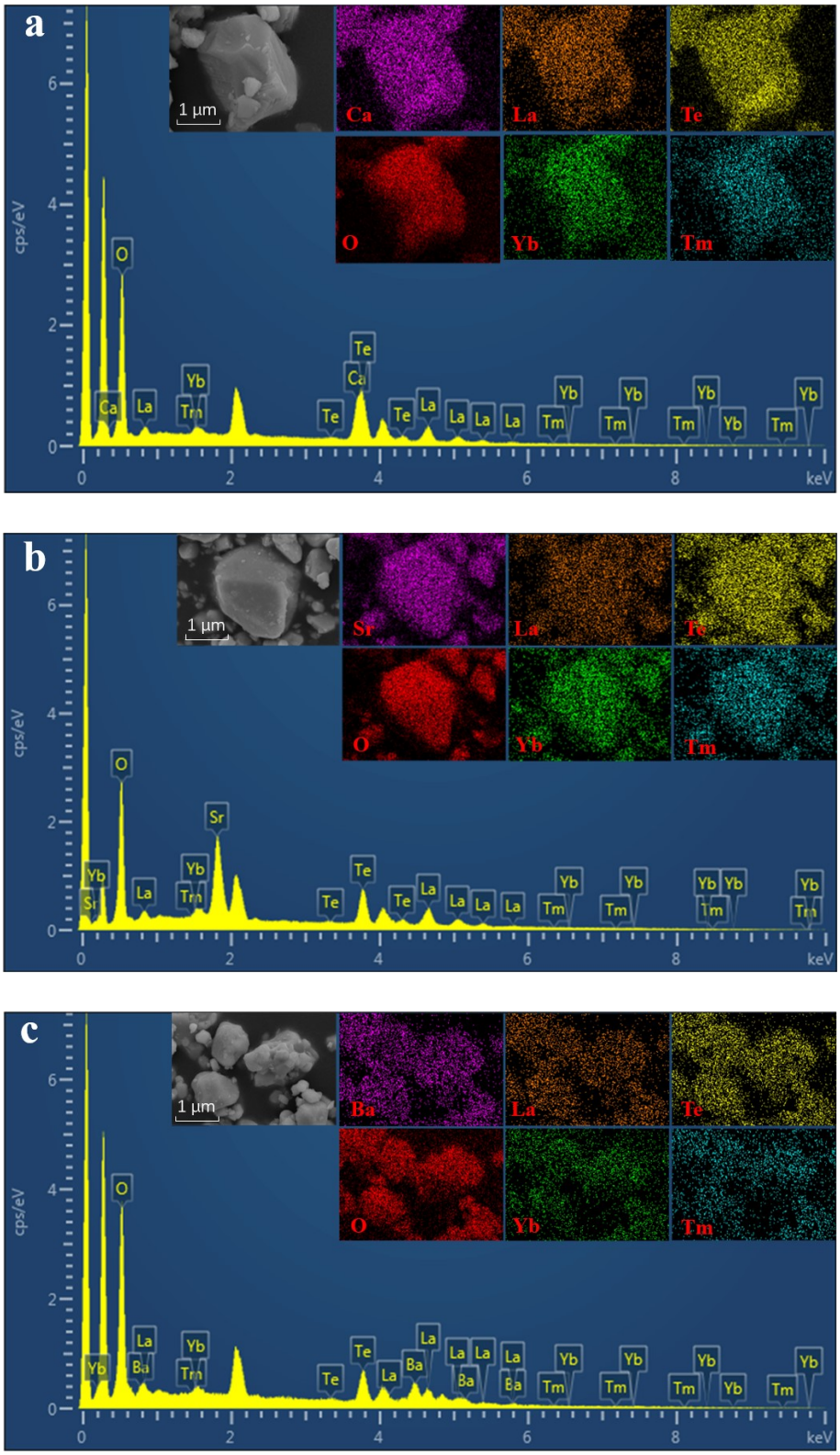


**Fig. S2.** SEM and elemental mapping images of the (a) $CaLaLiTeO_6$: 0.2% $Tm^{3+}$, 5% $Yb^{3+}$, (b) $SrLaLiTeO_6$: 0.2% $Tm^{3+}$, 5% $Yb^{3+}$, (c) $BaLaLiTeO_6$: 0.2% $Tm^{3+}$, 5% $Yb^{3+}$ phosphors.

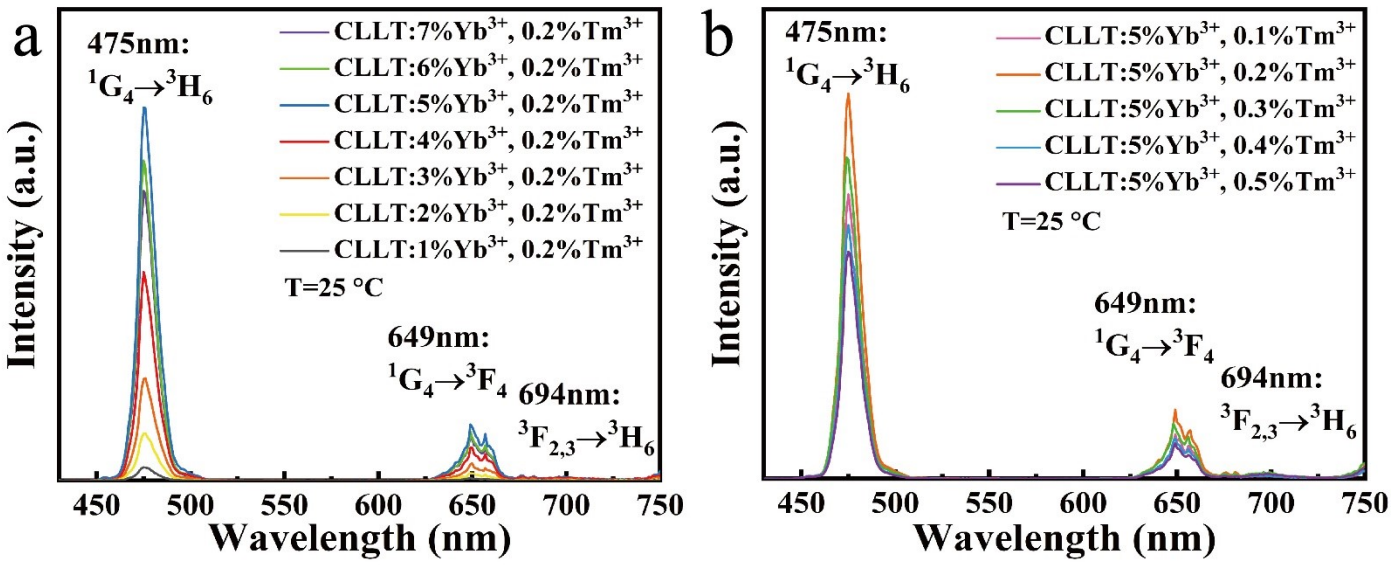


**Fig. S3.** (a and b) Emission spectra of $CaLaLiTeO_6$: x$Tm^{3+}$, 5%$Yb^{3+}$ and $CaLaLiTeO_6$: 0.2% $Tm^{3+}$, x$Yb^{3+}$ phosphors with diverse doping contents.

**The optimal doping concentration**

Use $CaLaLiTeO_6$: x$Yb^{3+}$, x$Tm^{3+}$ to study the optimal doping concentration of $Yb^{3+}$ and $Tm^{3+}$, fix the doping concentration of $Yb^{3+}$ and $Tm^{3+}$ in sequence, and change the concentration of another ion so as to cause a concentration gradient change. The PL spectra of $CaLaLiTeO_6$: x$Yb^{3+}$, 0.2% $Tm^{3+}$ excited by a 980nm light source are shown in Fig. S3a. In this system, concentration quenching occurs when x>5%. This is because with the continuous increase of $Yb^{3+}$ ion concentration, the sensitization of $Yb^{3+}$ to $Tm^{3+}$ is gradually replaced by reverse energy transfer [BET: $^2F_{7/2}(Yb^{3+})+{}^3H_4(Tm^{3+}) \rightarrow {}^2F_{5/2}(Yb^{3+})+{}^3H_6(Tm^{3+})$ or $^2F_{7/2}(Yb^{3+})+{}^3F_4(Tm^{3+}) \rightarrow {}^2F_{5/2}(Yb^{3+})+ {}^3H_6(Tm^{3+})$].The test results reveal that the luminescence intensity is optimal when the doping concentration of $Yb^{3+}$ is 5%. Then, fix the concentration of 5% $Yb^{3+}$, so that the concentration of $Tm^{3+}$ gradient changes from 0.1% to 0.5%. As shown in Fig.S3b, when the doping concentration of $Tm^{3+}$ is 0.2%, the emission intensity of the sample decreases with further increase of $Tm^{3+}$ concentration due to concentration quenching effect. Therefore, the optimal doping concentration of $CaLaLiTeO_6$ is 5% $Yb^{3+}$, 0.2% $Tm^{3+}$. In future studies, we will explore the optical properties of $SrLaLiTeO_6$ and $BaLaLiTeO_6$ based on this concentration.

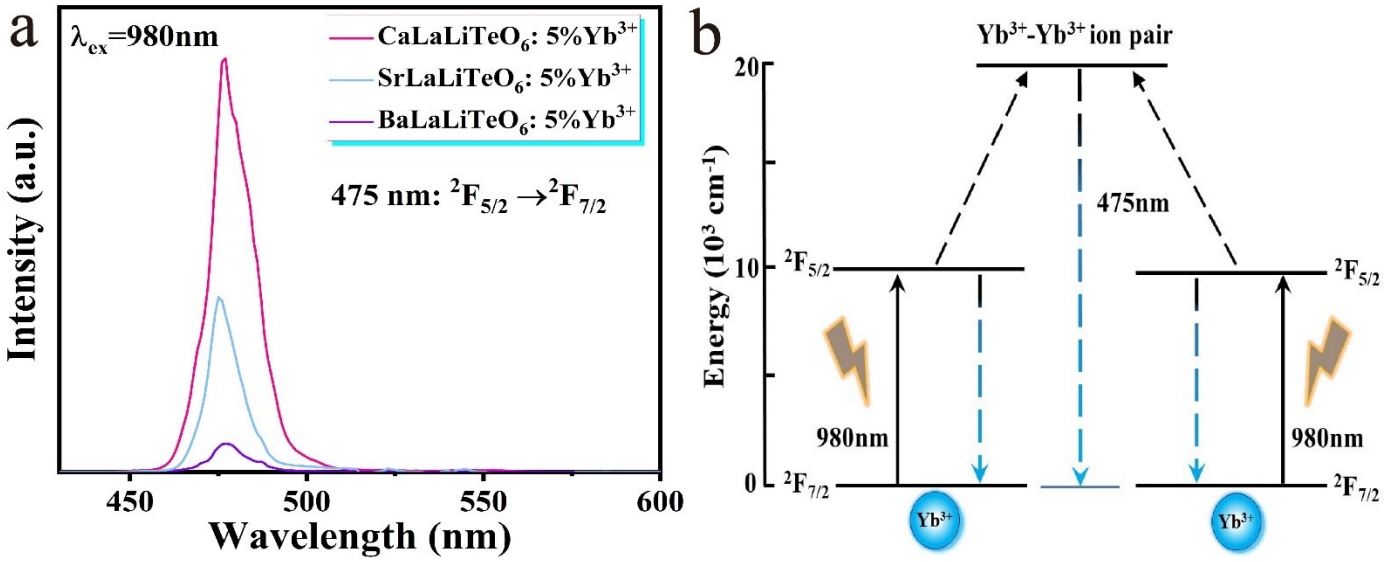


**Fig. S4.** (a) Up-conversion PL spectra of $ALaLiTeO_6$: 5% $Yb^{3+}$ (A = Ca, Sr, Ba) phosphor. (b) The energy level transition process diagram of $ALaLiTeO_6$: 5% $Yb^{3+}$phosphor.

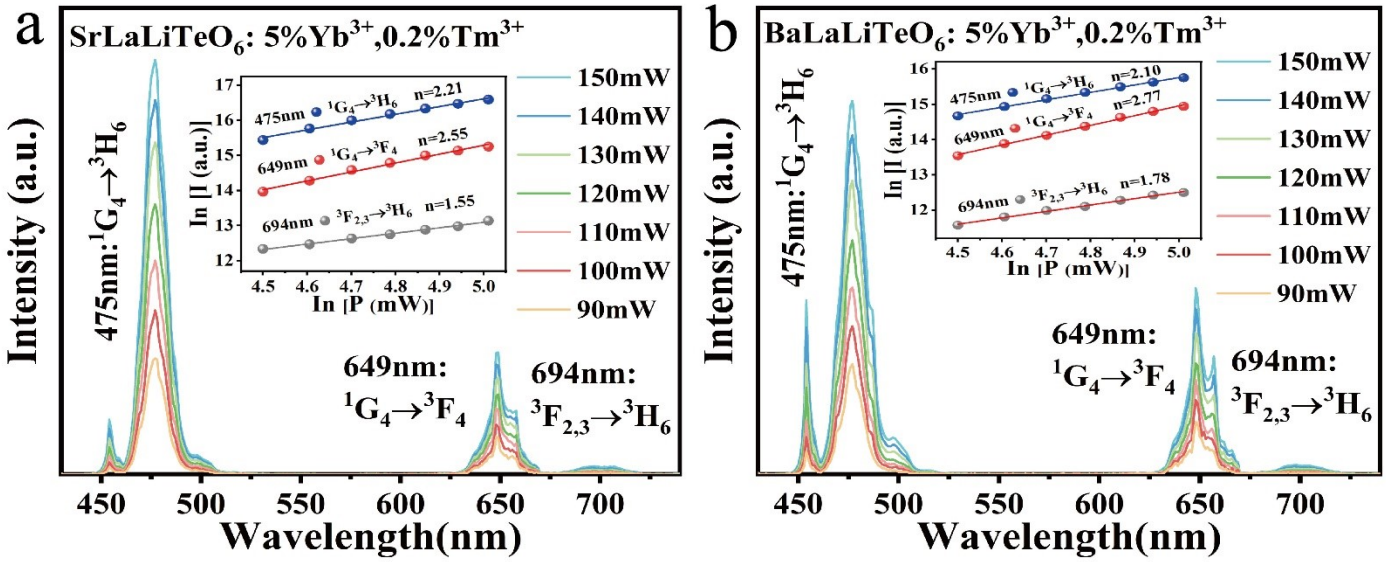


**Fig. S5.** The relationship between ln(I) and ln(P) of (a) $SrLaLiTeO_6$: 5% $Yb^{3+}$, 0.2% $Tm^{3+}$ and (b) $BaLaLiTeO_6$: 5% $Yb^{3+}$, 0.2% $Tm^{3+}$.

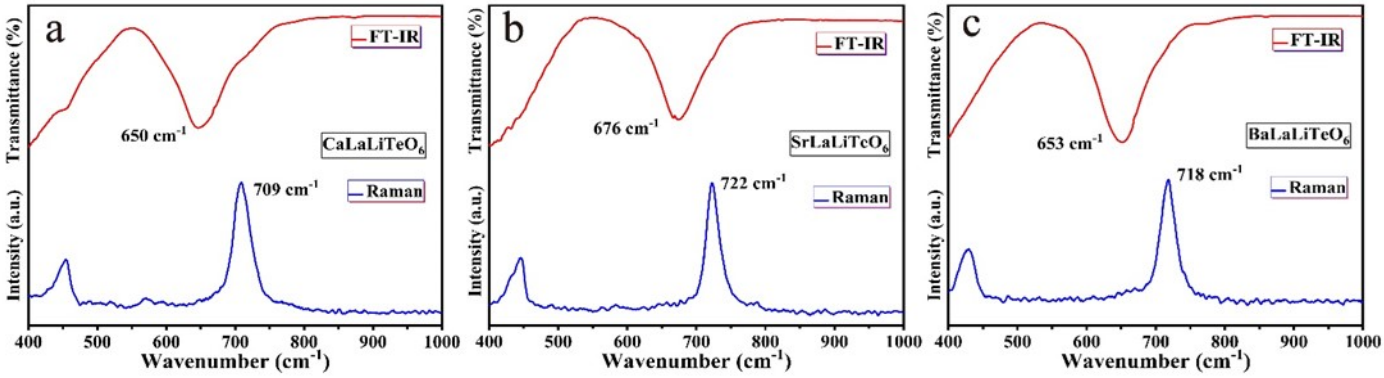


**Fig. S6.** FT-IR and Raman spectra of of (a) $CaLaLiTeO_6$: 5% $Yb^{3+}$, 0.2% $Tm^{3+}$ , (b) $SrLaLiTeO_6$: 5% $Yb^{3+}$, 0.2% $Tm^{3+}$ and (c) $BaLaLiTeO_6$: 5% $Yb^{3+}$, 0.2% $Tm^{3+}$ phosphor.

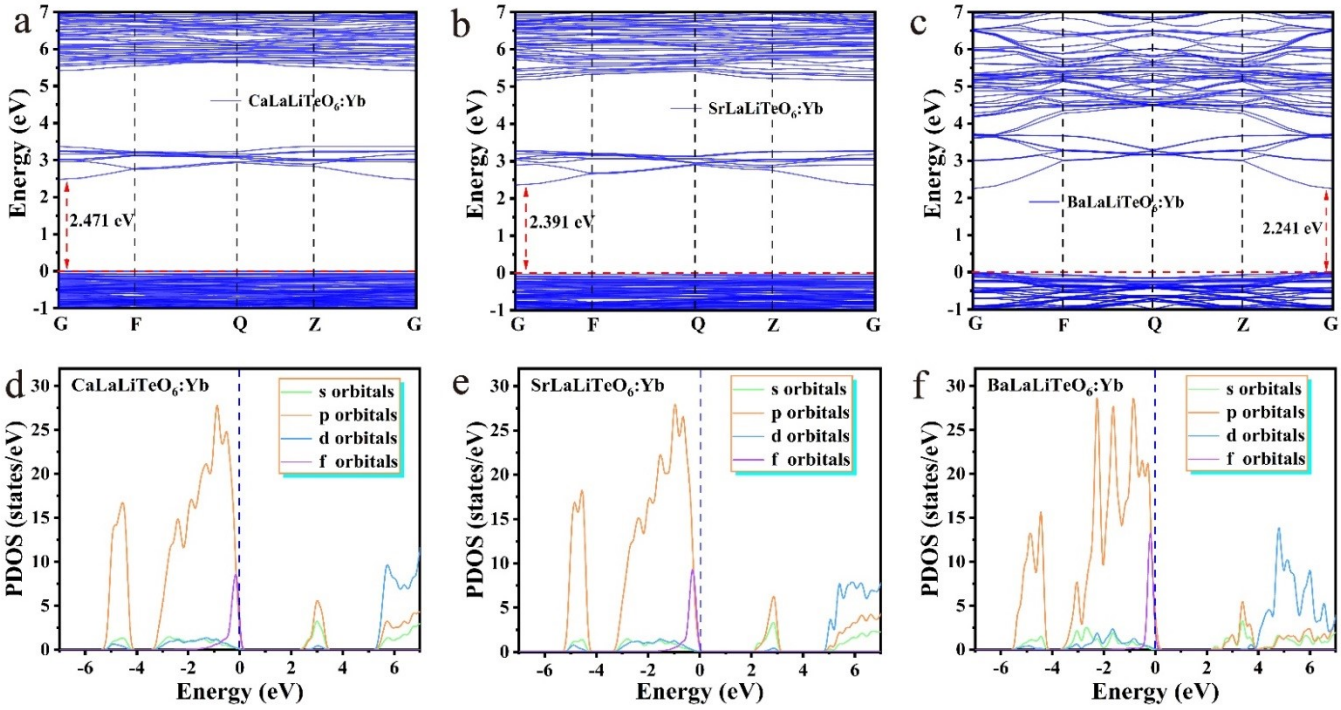


**Fig. S7.** Calculated band structure of (a) $CaLaLiTeO_6$: Yb, (b) $SrLaLiTeO_6$: Yb, (c) $BaLaLiTeO_6$: Yb. The PDOS, bonding and anti-bonding orbitals of (d) $CaLaLiTeO_6$: Yb, (e) $SrLaLiTeO_6$: Yb, (f) $BaLaLiTeO_6$: Yb.

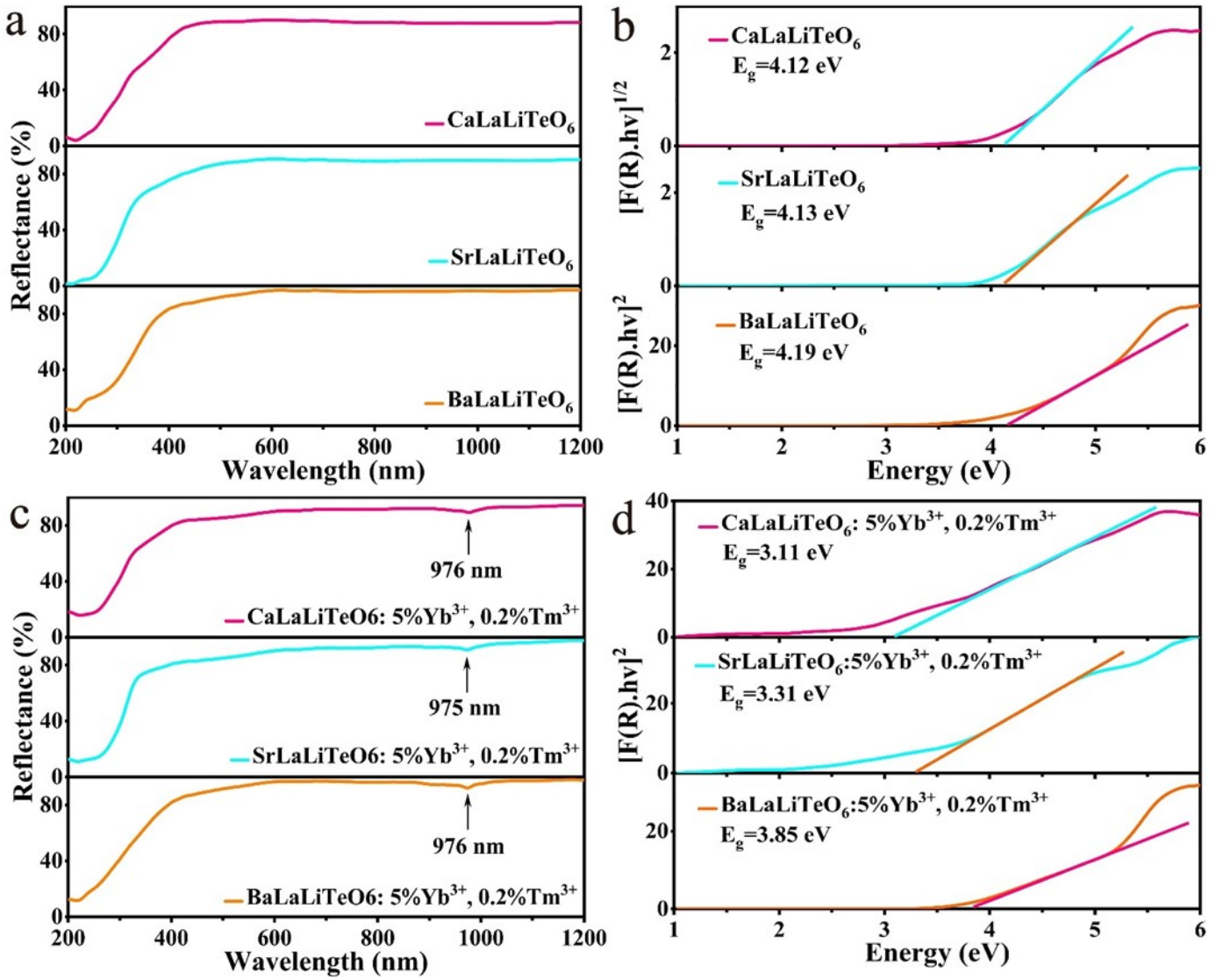


**Fig. S8.** UV-Vis-NIR absorption spectra of (a) matrix $ALaLiTeO_6$: (A = Ca, Sr, Ba) phosphors and (c) $ALaLiTeO_6$: 5 % $Yb^{3+}$, 0.2% $Tm^{3+}$ (A = Ca, Sr, Ba) phosphors in diffuse reflection mode; (b) and (d) Kubelka–Munk plots to estimate the optical band gap energies of the synthesized phosphors.

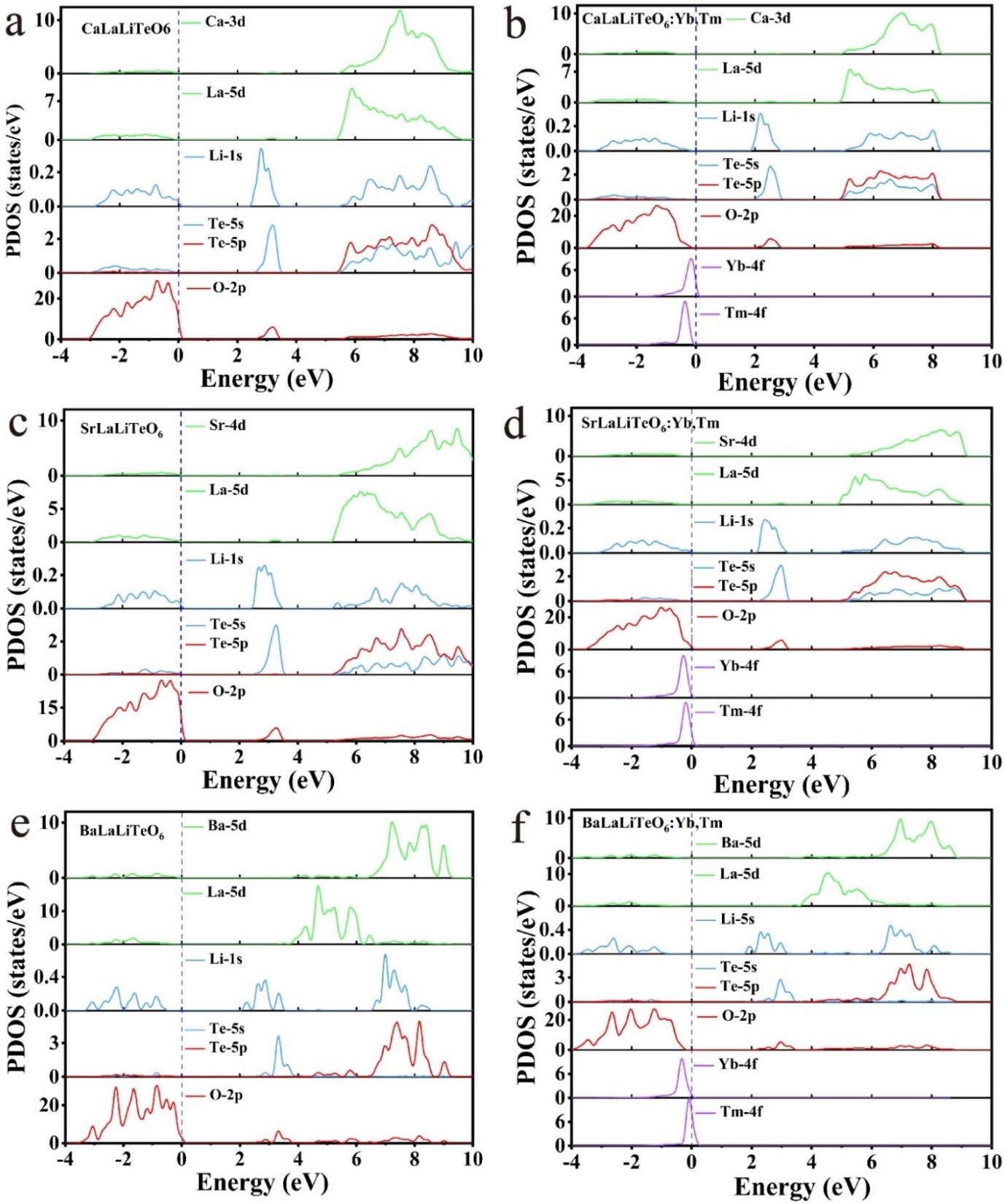


**Fig. S9.** Calculated partial density of states for (a) $CaLaLiTeO_6$, (b) $CaLaLiTeO_6$: Yb, Tm; (c) $SrLaLiTeO_6$, (d) $SrLaLiTeO_6$: Yb, Tm; (e) $BaLaLiTeO_6$, (f) $BaLaLiTeO_6$: Yb, Tm.

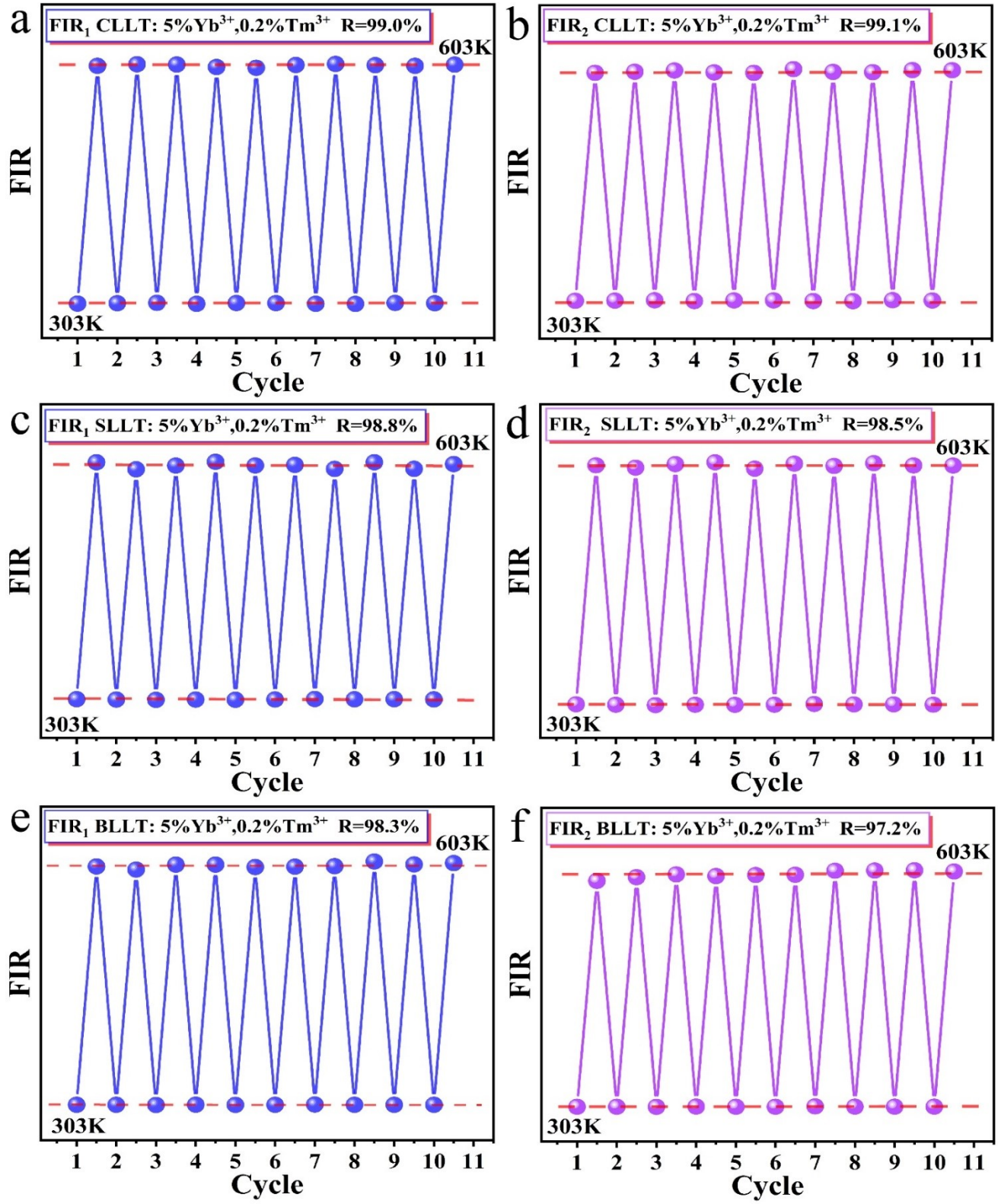


**Fig. S10.** (a-f) Repeatability heating-cooling cycles between 303 to 603 K of $ALaLiTeO_6$: 5% $Yb^{3+}$, 0.2% $Tm^{3+}$.

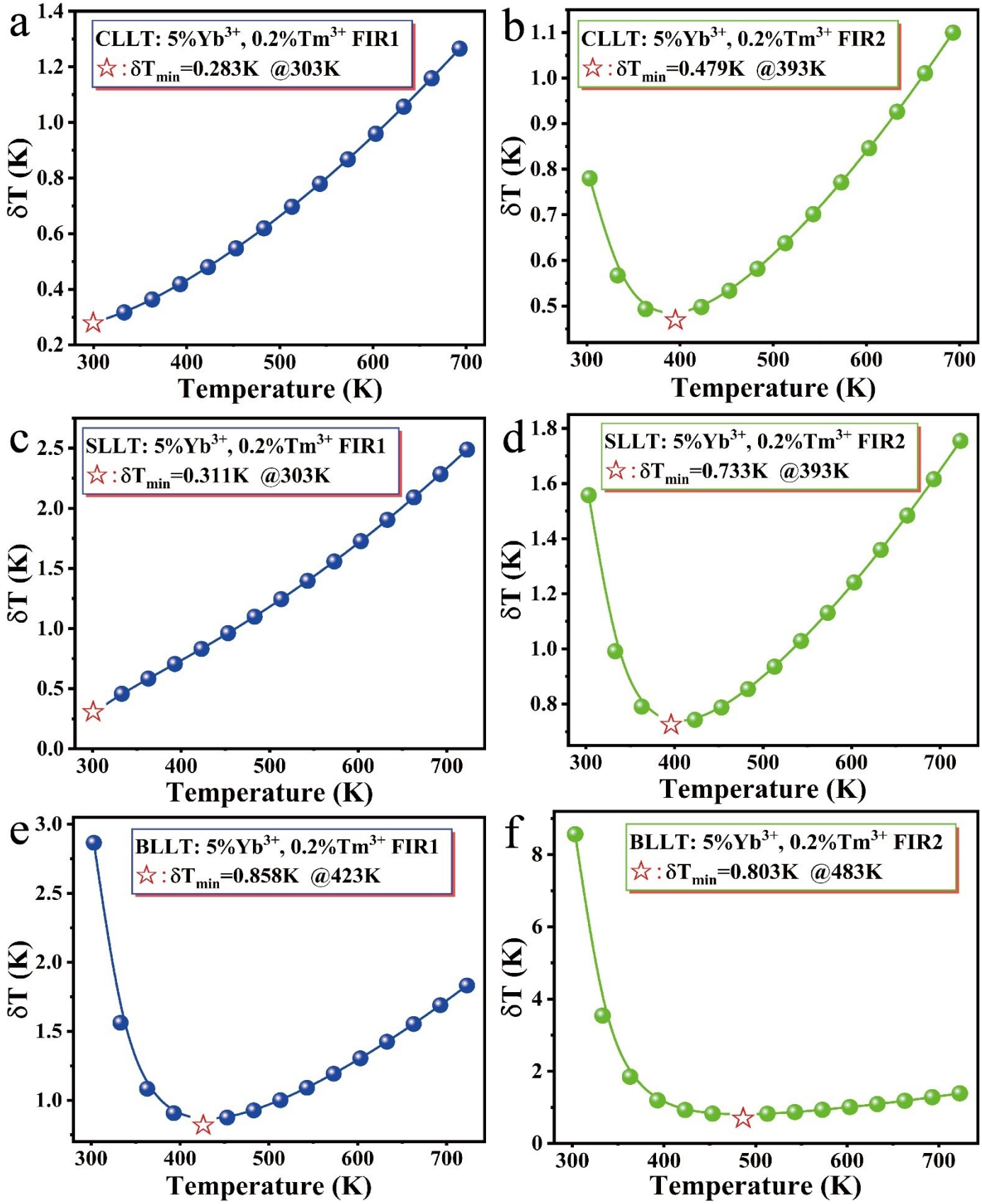


**Fig. S11.** (a-f) The calculation of δT results for $ALaLiTeO_6$: 5% $Yb^{3+}$, 0.2% $Tm^{3+}$.

# Supplementary Tables

**Table S1.** Refined crystallographic parameters of $CaLaLiTeO_6$: 5% $Yb^{3+}$, 0.2% $Tm^{3+}$.

| CLLT | Wyckoff sites | x | y | z | Occupancy |
|---|---|---|---|---|---|
| Ba1 | 4e | 0.15326 | 0.02467 | 0.24374 | 1.00000 |
| O1 | 4e | 0.24925 | 0.72378 | 0.04729 | 1.00000 |
| O2 | 4e | 0.24456 | 0.49054 | 0.24382 | 0.50000 |
| Ca3 | 4e | 0.26478 | 0.45069 | 0.25237 | 0.46900 |
| La4 | 4e | 0.32283 | 0.19227 | 0.04174 | 1.00000 |
| O5 | 2d | 0.50000 | 0.00000 | 0.50000 | 1.00000 |
| Li6 | 2a | 0.00000 | 0.00000 | 0.00000 | 1.00000 |
| Te7 | 4e | 0.26478 | 0.45069 | 0.25237 | 0.03000 |
| Yb8 | 4e | 0.26478 | 0.45069 | 0.25237 | 0.00100 |
| Tm9 | 4e | 0.15326 | 0.02467 | 0.24374 | 1.00000 |

**Table S2.** Refined crystallographic parameters of $SrLaLiTeO_6$: 5% $Yb^{3+}$, 0.2% $Tm^{3+}$.

| SLLT | Wyckoff sites | x | y | z | Occupancy |
|---|---|---|---|---|---|
| O1 | 4e | 0.10536 | 0.05909 | 0.23061 | 1.00000 |
| O2 | 4e | 0.24147 | 0.71703 | 0.07528 | 1.00000 |
| a3 | 4e | 0.26775 | 0.44071 | 0.25336 | 0.46900 |
| Sr4 | 4e | 0.26929 | 0.44222 | 0.25294 | 0.50000 |
| O5 | 4e | 0.34466 | 0.17223 | 0.05485 | 1.00000 |
| Li6 | 2d | 0.50000 | 0.00000 | 0.50000 | 1.00000 |
| Te7 | 2c | 0.00000 | 0.00000 | 0.00000 | 1.00000 |
| Yb8 | 4e | 0.26775 | 0.44071 | 0.25336 | 0.03000 |
| Tm9 | 4e | 0.26775 | 0.44071 | 0.25336 | 0.00100 |

**Table S3.** Refined crystallographic parameters of $BaLaLiTeO_6$: 5% $Yb^{3+}$, 0.2% $Tm^{3+}$.

| BLLT | Wyckoff sites | x | y | z | Occupancy |
|---|---|---|---|---|---|
| La1 | 4e | 0.25000 | 0.25000 | 0.25000 | 0.46900 |
| O2 | 2e | 0.23016 | 0.00000 | 0.00000 | 0.50000 |
| Ba3 | 4e | 0.25000 | 0.25000 | 0.25000 | 1.00000 |
| Li4 | 2d | 0.50000 | 0.50000 | 0.50000 | 1.00000 |
| Te5 | 2c | 0.00000 | 0.00000 | 0.00000 | 1.00000 |
| Yb6 | 4e | 0.25000 | 0.25000 | 0.25000 | 0.03000 |
| Tm7 | 4e | 0.25000 | 0.25000 | 0.25000 | 0.00100 |

**Table S4.** Table of cation radius differences for different substitutions.

| $R_s$ | $Ca^{2+}$(pm) | $Sr^{2+}$(pm) | $Ba^{2+}$(pm) | $La^{3+}$(pm) |
|---|---|---|---|---|
| r | 112 | 126 | 142 | 116 |
| $D_r$ ($Yb^{3+}$) | 12.1% | 21.8% | 30.6% | 15.1% |
| $D_r$ ($Tm^{3+}$) | 11.3% | 21.1% | 30% | 14.3% |

**Table S5.** Energy value of simplified energy levels to the ground level for $Tm^{3+}$ ions, and the energy gap of selected transitions in $Tm^{3+}$.

| Energy level | Energy($cm^{-1}$) | Transition | $\Delta E$($cm^{-1}$) |
|---|---|---|---|
| $^1D_2$ | 28010 | NR1:$^3H_5 \rightarrow {}^3F_4$ | 2510 |
| $^1G_4$ | 21450 | NR2:$^3F_{2,3} \rightarrow {}^3H_4$ | 1530~2030 |
| $^3F_2$ | 14800 | CR1:$^3H_4 \rightarrow {}^1D_2$ | -15240 |
| $^3F_3$ | 14300 | CR1:$^1G_4 \rightarrow {}^3F_4$ | 15830 |
| $^3H_4$ | 12770 | CR2:$^1G_4 \rightarrow {}^1D_2$ | -6560 |
| $^3H_5$ | 8430 | CR2:$^3H_4 \rightarrow {}^3F_4$ | 6850 |
| $^3F_4$ | 5920 | CR3:$^1G_4 \rightarrow {}^3F_{2,3}$ | 6650~7150 |
| $^3H_6$ | 0 | CR3:$^3H_6 \rightarrow {}^3F_4$ | -5920 |

**Table S6.** Thermometry sensitivity of $Yb^{3+}$ and $Tm^{3+}$ co-doped up-conversion phosphors.

| Phosphors | Transitions | Temperature (K) | $S_a$ (% $K^{-1}$) | $S_r$ (% $K^{-1}$) | Refs |
|---|---|---|---|---|---|
| $Sr_2GdF_7$: $Tm^{3+}/Yb^{3+}$ | $^3F_{2,3}\rightarrow {}^3H_6/{}^1G_4\rightarrow {}^3F_4$ | 293-563 | 3.9 | 1.97 | 1 |
| $NaY_2F_7$:$Yb^{3+}/Tm^{3+}$ | $^3F_{2,3}\rightarrow {}^3H_6/{}^1G_4\rightarrow {}^3F_4$ | 307-567 | 10.01 | 1.63 | 2 |
| $SrF_2$:$Tm^{3+}/Yb^{3+}$ | $^3H_4\rightarrow {}^3H_6/{}^1G_4\rightarrow {}^3H_6$ | 298–573 | 0.21 | 2.2 | 3 |
| $Bi_2SiO_5$:$Tm^{3+}/Yb^{3+}$@$SiO_2$ | $^1G_4\rightarrow {}^3F_4/{}^3F_{2,3}\rightarrow {}^3H_4$ | 280-400 | 1.68 | 1.95 | 4 |
| $La_2MgTiO_6$:$Tm^{3+}$, $Yb^{3+}$ | $^3F_{2,3}\rightarrow {}^3H_6/{}^1G_4\rightarrow {}^3F_4$ | 313-573 | 4.94 | 1.92 | 5 |
| | $^3F_{2,3}\rightarrow {}^3H_6/{}^1G_4\rightarrow {}^3H_6$ | 313-573 | 3.32 | 1.63 | |
| $La_2Mo_2O_9$: $Tm^{3+}$, $Yb^{3+}$ | $^3F_{2,3}\rightarrow {}^3H_6/{}^3H_4\rightarrow {}^3H_6$ | 293–553 | 0.284 | 2.29 | 6 |
| $Ba_3Y_4O_9$:$Yb^{3+}/Tm^{3+}$ | $^3F_{2,3}\rightarrow {}^3H_6/{}^1G_4\rightarrow {}^3H_6$ | 294-573 | 0.81 | 1.08 | 7 |
| $Sr_3Y(PO_4)_3$: $Tm^{3+}/Yb^{3+}$ | $^3F_{2,3}\rightarrow {}^3H_6/{}^1G_4\rightarrow {}^3F_4$ | 298–573 | 1.27 | 1.52 | 8 |
| $Ba_{3-x}Sr_xLu_4O_9$: $Tm^{3+}/Yb^{3+}$ | $^1G_4\rightarrow {}^3F_4$ /$^3F_3\rightarrow {}^3H_6$ | 303-573 | 1.50 | 0.88 | 9 |
| $Ca_9Y(PO_4)_7$: $Tm^{3+}$, $Yb^{3+}$ | $^3F_{2,3}\rightarrow {}^3H_6/{}^1G_4\rightarrow {}^3F_4$ | 323–823 | 8.07 | 1.07 | 10 |
| $CaIn_2O_4$: $Tm^{3+}/Yb^{3+}$ | $^3H_4\rightarrow {}^3H_6/{}^1G_4\rightarrow {}^3H_6$ | 303-373 | 1.0 | 0.51 | 11 |
| $Y_2O_3$: $Tm^{3+}/Yb^{3+}$ | $^3H_4\rightarrow {}^3H_6/{}^1G_4\rightarrow {}^3H_6$ | 303-573 | 11.7 | 1.51 | 12 |
| $Y_2Mo_3O_{12}$: $Tm^{3+}$/0.26$Yb^{3+}$ | $^3F_{2,3}\rightarrow {}^3H_6/{}^1G_4\rightarrow {}^3F_4$ | 303-583 | 19.8 | 2.46 | 13 |
| | $^3F_{2,3}\rightarrow {}^3H_6/{}^1G_4\rightarrow {}^3H_6$ | 303-583 | 3.17 | 3.27 | |
| $Y_2Mo_3O_{12}$: $Tm^{3+}$/0.14$Yb^{3+}$ | $^3F_{2,3}\rightarrow {}^3H_6/{}^1G_4\rightarrow {}^3F_4$ | 303-503 | 13.1 | 2.67 | |
| | $^3F_{2,3}\rightarrow {}^3H_6/{}^1G_4\rightarrow {}^3H_6$ | 303-503 | 2.13 | 3.06 | |
| $BaLu_6(Ge_2O_7)_2(Ge_3O_{10})$ | $^3F_{2,3}\rightarrow {}^3H_6/{}^3H_4\rightarrow {}^3H_6$ | 298-498 | 2.1 | 1.94 | 14 |
| $SrWO_4$: $Tm^{3+}/Yb^{3+}$ | $^3F_{2,3}\rightarrow {}^3H_6/{}^3H_4\rightarrow {}^3H_6$ | 308-573 | 0.617 | 0.7 | 15 |
| $NaYTiO_4$: $Tm^{3+}/Yb^{3+}$ | $^3F_{2,3}\rightarrow {}^3H_6/{}^3H_4\rightarrow {}^3H_6$ | 463-823 | 3.2 | 1.04 | 16 |
| $LaPO_4$: $Tm^{3+}/Yb^{3+}$ | $^3F_{2,3}\rightarrow {}^3H_6/{}^3H_4\rightarrow {}^3H_6$ | 293-773 | 2.5 | 3.0 | 17 |
| $Bi_2Ti_2O_7$: $Tm^{3+}/Yb^{3+}$ | $^3F_{2,3}\rightarrow {}^3H_6/{}^3H_4\rightarrow {}^3H_6$ | 300-505 | / | 2.4 | 18 |
| $CaLaLiTeO_6$: 5%$Yb^{3+}$, 0.2%$Tm^{3+}$ | $^3F_{2,3}\rightarrow {}^3H_6/{}^1G_4\rightarrow {}^3F_4$ | 303-693 | 3.19 | 2.11 | This Work |
| $SrLaLiTeO_6$: 5%$Yb^{3+}$, 0.2%$Tm^{3+}$ | | | 8.52 | 4.69 | |
| $BaLaLiTeO_6$: 5%$Yb^{3+}$, 0.2%$Tm^{3+}$ | | | 10.05 | 1.29 | |
| $CaLaLiTeO_6$: 5%$Yb^{3+}$, 0.2%$Tm^{3+}$ | $^3F_{2,3}\rightarrow {}^3H_6/{}^1G_4\rightarrow {}^3H_6$ | | 1.19 | 1.22 | |
| $SrLaLiTeO_6$: 5%$Yb^{3+}$, 0.2%$Tm^{3+}$ | | | 2.83 | 1.35 | |
| $BaLaLiTeO_6$: 5%$Yb^{3+}$, 0.2%$Tm^{3+}$ | | | 5.87 | 1.22 | |

**References**


1 W. Chen, J. Cao, F. Hu, R. Wei, L. Chen and H. Guo, $Sr_2GdF_7$:$Tm^{3+}$/$Yb^{3+}$ glass ceramic: A highly sensitive optical thermometer based on FIR technique, *Journal of Alloys and Compounds*, 2018, **735**, 2544-2550.

2 S. Chen, W. Song, J. Cao, F. Hu and H. Guo, Highly sensitive optical thermometer based on FIR technique of transparent $NaY_2F_7$:$Tm^{3+}$/$Yb^{3+}$ glass ceramic, *Journal of Alloys and Compounds*, 2020, **825**, 154011.

3 N. Rakov, S. A. Vieira and A. S. L. Gomes, $Tm^{3+}$/$Yb^{3+}$co-doped $SrF_2$ up-conversion phosphors for non-invasive optical thermometry: ratiometric approach using thermal and non-thermal coupled fluorescent emission bands, *Applied Physics A*, 2021, **127**.

4 E. Casagrande, M. Back, D. Cristofori, J. Ueda, S. Tanabe, S. Palazzolo, F. Rizzolio, V. Canzonieri, E. Trave and P. Riello, Upconversion-mediated Boltzmann thermometry in double-layered $Bi_2SiO_5$:$Yb^{3+}$,$Tm^{3+}$@$SiO_2$ hollow nanoparticles, *Journal of Materials Chemistry C*, 2020, **8**, 7828-7836.

5 K. Zhu, H. Xu, Z. Wang and Z. Fu, Lanthanide-doped lead-free double perovskite $La_2MgTiO_6$ as ultra-bright multicolour LEDs and novel self-calibrating partition optical thermometer, *Inorganic Chemistry Frontiers*, 2023, DOI: 10.1039/d3qi00529a, 3383-3395.

6 Q. Xiao, X. Dong, X. Yin, H. Wang, H. Zhong, K. Liu, B. Dong and X. Luo, Promising $Yb^{3+}$-sensitized $La_2Mo_2O_9$ phosphors for multi-color up-conversion luminescence and optical temperature sensing, *Journal of Alloys and Compounds*, 2022, **895**, 162686.

7 S. Liu, J. Cui, J. Jia, J. Fu, W. You, Q. Zeng, Y. Yang and X. Ye, High sensitive $Ln^{3+}$/$Tm^{3+}$/$Yb^{3+}$ ($Ln^{3+}$ = $Ho^{3+}$, $Er^{3+}$) tri-doped $Ba_3Y_4O_9$ upconverting optical thermometric materials based on diverse thermal response from non-thermally coupled energy levels, *Ceramics International*, 2019, **45**, 1-10.

8 W. Liu, X. Wang, Q. Zhu, X. Li, X. Sun and J.-G. Li, Upconversion luminescence and favorable temperature sensing performance of eulytite-type $Sr_3Y(PO_4)_3$:$Yb^{3+}$/$Ln^{3+}$ phosphors (Ln=Ho, Er, Tm), *Science and Technology of Advanced Materials*, 2019, **20**, 949-963.

9 X. Zhang, H. Zheng, J. Hu, F. Lu, X. Peng, R. Wei, F. Hu and H. Guo, Enhanced up-conversion luminescence and temperature sensing property of Ba Sr $Lu_4O_9$:$Tm^{3+}$/$Yb^{3+}$ phosphors, *Ceramics International*, 2021, **47**, 32290-32296.

10 Y. Zhuang, D. Wang and Z. Yang, Upconversion luminescence and optical thermometry based on non-thermally-coupled levels of $Ca_9Y(PO_4)_7$: $Tm^{3+}$, $Yb^{3+}$ phosphor, *Optical Materials*, 2022, **126**, 112167.

11 H. Liu, Z. Zhang, J. Liu, K. Wang and Y. Zhang, Efficient upconversion and downshifting luminescence of $CaIn_2O_4$: $Yb^{3+}$/$Tm^{3+}$/$RE^{3+}$ (RE=Er/Ho) phosphor: Temperature sensing performance in the visible and near-infrared range, *Ceramics International*, 2023, **49**, 30510-30521.

12 V. Lojpur, M. Nikolic, L. Mancic, O. Milosevic and M. D. Dramicanin, $Y_2O_3$:Yb,Tm and $Y_2O_3$:Yb,Ho powders for low-temperature thermometry based on up-conversion fluorescence, *Ceramics International*, 2013, **39**, 1129-1134.

13 H. Lv, P. Du, W. Li and L. Luo, Tailoring of Upconversion Emission in $Tm^{3+}/Yb^{3+}$-Codoped $Y_2Mo_3O_{12}$ Submicron Particles Via Thermal Stimulation Engineering for Non-invasive Thermometry, *ACS Sustainable Chemistry & Engineering*, 2022, **10**, 2450-2460.

14 O. A. Lipina, L. L. Surat, A. Y. Chufarov, I. V. Baklanova, A. N. Enyashin, M. A. Melkozerova, A. P. Tyutyunnik and V. G. Zubkov, Structural, electronic and optical properties of $BaRE_6(Ge_2O_7)_2(Ge_3O_{10})$ (RE = Tm, Yb, Lu) compounds and $BaYb_6(Ge_2O_7)_2(Ge_3O_{10})$:$Tm^{3+}$ and $BaLu_6(Ge_2O_7)_2(Ge_3O_{10})$:$Yb^{3+}$,$Tm^{3+}$ phosphors: potential applications in temperature sensing, *Dalton Transactions*, 2023, **52**, 7482-7494.

15 H. Song, C. Wang, Q. Han, X. Tang, W. Yan, Y. Chen, J. Jiang and T. Liu, Highly sensitive $Tm^{3+}/Yb^{3+}$ codoped $SrWO_4$ for optical thermometry, *Sensors and Actuators A: Physical*, 2018, **271**, 278-282.

16 Y. Wang, Y. Li, C. Ma, Z. Wen, X. Yuan and Y. Cao, Temperature sensing properties of $NaYTiO_4$: Yb/Tm phosphors based on near-infrared up-conversion luminescence, *Journal of Luminescence*, 2022, **248**, 118917.

17 A. Tymiński, E. Śmiechowicz, I. R. Martín and T. Grzyb, Ultraviolet- and Near-Infrared-Excitable $LaPO_4$:$Yb^{3+}/Tm^{3+}/Ln^{3+}$ (Ln = Eu, Tb) Nanoparticles for Luminescent Fibers and Optical Thermometers, *ACS Applied Nano Materials*, 2020, **3**, 6541-6551.

18 W. Ge, M. Xu, J. Shi, J. Zhu and Y. Li, Highly temperature-sensitive and blue upconversion luminescence properties of $Bi_2Ti_2O_7$:$Tm^{3+}/Yb^{3+}$ nanofibers by electrospinning, *Chemical Engineering Journal*, 2020, **391**, 123546.